Pergamon

Int. J. Heat Mass Transfer. Vol. 41, No. 1, pp. 229–239, 1998

Printed in Great Britain
0017-9310/98 $19.00+0.00

PII: S0017-9310(96)00160-3

Transient response of the human limb to an external stimulust

WILFRIED ROETZEL
Institut für Thermodynamik, Universität der Bundeswehr Hamburg, D-22039 Hamburg, Germany

and

YIMIN XUAN
College of Power Engineering, Nanjing University of Science & Technology, Nanjing, People's Republic of China

(*Received* 9 *February* 1996 *and in final form* 7 *May* 1996)

Abstract—The multidimensional transient temperature profiles of the arterial and venous blood flows and of the tissue within a limb are simulated with the bioheat equations developed by means of the heat transfer principle in porous media. The conjugated differential equations are solved numerically. Three different layer models are introduced to treat discrete distributions of the anatomical and thermal properties. Some examples are computed and discussed. © 1997 Elsevier Science Ltd.

INTRODUCTION

Heat transport within the human body is a complicated process involving metabolic heat generation, heat conduction in tissue, convection and perfusion of the arterial-venous blood through the capillary bed and interaction with the environment. The accurate description of the human thermal system is necessary for development of biological and medical technology. Bioheat transfer affects the behaviour of biological systems. To some extent, the bioheat transfer model of the human body is the basis of thermotherapy, the human thermoregulation system and design of heating or cooling garments. With the human bioheat transfer model, one can predict the effects of a harsh (hot or cold) environment on the physiological processes of the human being, which helps in better utilization of manpower and prevention of disease and accidents [1].

An acceptable model should account for the following factors: heat conduction in the tissue, heat convection and perfusion of the blood, heat storage in the blood and tissue, metabolic heat generation, thermal and anatomical properties of organs and tissues, geometry of the organism and interaction with the environment. If the model is applied to thermoregulation, physiological properties and functions of the human body need to be included. Since the appearance of Pennes' bioheat equation [2], plenty of publications have been devoted to the thermal modelling of the human body. Charny [3] gave a detailed review of the chronological development of mathematical models of bioheat transfer. In principle, most of the bioheat transfer models described in ref. [3] are extended or modified versions of the original work of Pennes and the fundamental structure of these models remains the same.

For solving heat transfer problems within the human body, the body was artificially divided into a few parts such as the head, the trunk and the limbs. Thermal coupling among different body parts was established by the lumped-parameter equation of the blood flow. The heterogeneity of the tissue and tortuosity of the vessels are two important features with respect to heat transport. Generally, anatomical investigation gives the averaged values of thermal and physiological properties and no detailed spatial distributions of these properties. To take local variation of thermal properties of the tissue and metabolic heat generation within the tissue into account, the so-called 'core and shell' model [1] and 'four-layer' model [4] were developed for the thermoregulatory application, in which temperature changes of both arterial and venous blood flows were treated by the lumped-parameter model. Usually the bioheat equation is solved in the radial or both the radial and tangential directions in order to avoid mathematical complexity, but it does not mean that axial heat transfer and temperature gradient are neglectable. In fact, temperature variation in the axial direction is greater than that in the radial direction because of the blood perfusion

†Dedicated to Academician Professor Alexandr Ivanovich Leontiev on the occasion of his 70th birthday.

NOMENCLATURE

a	thermal diffusivity [$m^2 s^{-1}$]
A	surface [m^2]
c	specific heat capacity [$J kg^{-1} K^{-1}$]
d^*	hydraulic diameter [m]
h	local volumetric heat transfer coefficient [$W m^{-3} K^{-1}$]
h_m	mass transfer coefficient [$m s^{-1}$]
$\mathbf{k}$	thermal conductivity tensor
L	length of the limb [m]
Nu	Nusselt number
q	metabolic heat source [$W m^{-3}$]
R	radius [m]
T	temperature [°C]
$\langle T\rangle$	local volume-averaged temperature [°C]
$\mathbf{u}$	velocity tensor
u	velocity [$m s^{-1}$].

Greek symbols

ε	porosity
γ_{fg}	latent heat of vaporisation of water [$J kg^{-1}$]
ρ	density [$kg m^{-3}$]
σ	specific surface area [$m^2 m^{-3}$]
τ	time [s].

Superscripts

a	arterial blood
b	blood phase
s	solid tissue
v	venous blood.

Subscripts

a	arterial blood
b	blood phase
m	metabolism
s	solid tissue
v	venous blood
w	water.

through the tissue and the countercurrent effect between the arterial and venous blood flows [5].

As pointed out by Weinbaum *et al.* [6], the fundamental difficulty in modelling heat transfer processes within the human body is incorporation of the complex vascular architecture, e.g. dramatic variation in number, size, spacing of the vessels, thermal interaction among arteries, veins and tissues, convection and perfusion of the blood through the tortuous capillary beds, metabolic heat generation and interaction with the environment into a complete model. In their series of papers, Weinbaum *et al.* [7–9] proposed a new bioheat equation which is based on some anatomical understanding. Considering variation of the number density and size and flow velocity of the countercurrent arterio-venous vessels, they put forward some examples of steady-state heat transfer. This model may be useful in describing temperature distribution in a single organ, but it will be awkward to apply it to the whole human body for thermoregulation. Detailed argument on this model was given by Wissler [10].

In a previous article [5] the tissue was treated as a porous medium and the fundamental principle of heat transfer in porous media was applied to modelling thermal process within the human body. Without the assumption of the local thermal equilibrium between the blood and the tissue, a two-medium treatment of the single-phase flow and heat transfer was involved. The effective thermal conductivity is used in order to take thermal dispersion of the blood through the tissue into account. Based on the continuum assumption, two equations were derived for the blood and the tissue, respectively:

$$\varepsilon(\rho c_p)_b\left[\frac{\partial\langle T\rangle^b}{\partial\tau}+\langle\mathbf{u}\rangle^b\cdot\nabla\langle T\rangle^b\right]$$
$$=\nabla\cdot[\mathbf{k}_b^a\cdot\nabla\langle T\rangle^b]+h_{bs}(\langle T\rangle^s-\langle T\rangle^b) \quad (1)$$

$$(1-\varepsilon)(\rho c_p)_s\frac{\partial\langle T\rangle^s}{\partial\tau}=\nabla\cdot[\mathbf{k}_s^a\cdot\nabla\langle T\rangle^s]$$
$$+h_{sb}(\langle T\rangle^s-\langle T\rangle^b)+q_m(1-\varepsilon). \quad (2)$$

If sufficient information about the thermal and anatomical properties of the human body as well as the velocity and direction of the blood are at hand, both these equations can be used directly to determine temperature distributions. In the absence of detailed information, these two equations may be simplified to make simulation of the human thermal system tractable. In view of this fact, the dispersed plug-flow model was applied to steady-state temperature simulation of the arm [5]. As illustrated by the examples, the temperature slope of the tissue in the axial direction is steeper than that in the radial direction, which may partly explain the reason why the foot and hand have lower temperatures than the other parts.

This article applies the bioheat equations developed in the previous work [5] to simulating a transient response of the limb to external stimulus. The two-dimensional heat transport equations are proposed for the tissue, the arterial and venous blood flows. These equations are conjugated by interstitial heat

exchange between the tissue and the blood. To describe the convective heat transfer, the interstitial convection heat transfer term $h_{bs}(\langle T\rangle^s-\langle T\rangle^b)$ or $h_{sb}(\langle T\rangle^b-\langle T\rangle^s)$, rather than the term $u_b\rho_b c_{pb}(T_a-T_s)$ which was used in most of the existing publications, is assumed. Heat conduction within the solid tissue in both the axial and radial directions and the countercurrent effect between the arterial and venous blood flows are involved. As the first step, the passive thermal system is treated. One of the thermoregulatory functions of the human body exposed to a hot environment, heat loss by sweating, is taken into account in the model by introducing an appropriate boundary condition. The incorporation of other thermoregulatory functions of the human body into the whole thermal human system will be handled in another article.

MATHEMATICAL FORMULATION

From equations (1) and (2), one can easily obtain the transient heat transfer equations for a limb. In a similar way to the procedure of deriving the steady-state heat equations [5], the following differential equations in the cylinder coordinate system are obtained:

$$\varepsilon_a(\rho c_p)_a\left(\frac{\partial\langle T\rangle^a}{\partial\tau}+u_a\frac{\partial\langle T\rangle^a}{\partial x}\right)=\frac{\partial}{\partial x}\left(k_a^*\frac{\partial\langle T\rangle^a}{\partial x}\right)+h_{bs}(\langle T\rangle^s-\langle T\rangle^b) \quad (3)$$

$$\varepsilon_v(\rho c_p)_v\left(\frac{\partial\langle T\rangle^v}{\partial\tau}-u_v\frac{\partial\langle T\rangle^v}{\partial x}\right)=\frac{\partial}{\partial x}\left(k_v^*\frac{\partial\langle T\rangle^v}{\partial x}\right)+h_{vs}(\langle\bar{T}\rangle^s-\langle T\rangle^v) \quad (4)$$

$$(1-\varepsilon)(\rho c_p)_s\frac{\partial\langle T\rangle^s}{\partial\tau}=\frac{\partial}{\partial x}\left(k_v^*\frac{\partial\langle T\rangle^v}{\partial x}\right)+\frac{1}{r}\frac{\partial}{\partial r}\left(k_s^*\frac{\partial\langle T\rangle^s}{\partial r}\right)+q_m(1-\varepsilon)+h_{sb}(\langle T\rangle^s-\langle T\rangle^b)+h_{sb}(\langle T\rangle^s-\langle T\rangle^b) \quad (5)$$

where $\langle\bar{T}\rangle^s$ is the tissue temperature averaged over the transverse section of the limb at any axial position x and $\varepsilon=\varepsilon_a+\varepsilon_v$.

Equations (3)–(5) are valid for the arterial and venous blood flows and the tissue, respectively. All thermal and physiological parameters involved in these equations are allowed to be spatially and temporally distributed functions, for example the blood velocities u_a and u_v are allowed to be functions of both variables x and r (e.g. symmetrical parabolic distributions). If the averaged values of u_a and u_v are assumed, equations (3) and (4) actually represent the dispersed plug-flow model. The countercurrent effect between the arterial and venous blood flows is expressed by the second term on the left-hand side of both equations (3) and (4). The equivalent (or effective) thermal conductivities k_a^* and k_v^* are used to account for the thermal dispersion of the blood through the porous tissue. Computation has shown that the temperature simulation remains almost the same, whether the governing equations for both the blood flows are one-dimensional or two-dimensional. Therefore, here the one-dimensional model is applied to the blood. In addition, the dispersed model applied to the blood flow can compensate for deviation of the one-dimensional model from the two-dimensional one, which is one of the merits of the dispersed model that finds wide use in chemical and thermal engineering.

The metabolic heat generation is taken into account in equation (5). The terms of interstitial heat exchange between the blood and the tissue appear in the three equations mentioned above which are then conjugated. The metabolic heat generation of the blood flow as well as the heat exchange between the blood and the tissue are two main ways of controlling and regulating the temperature of the human body subject to an external hot or cold stimulus. In the absence of detailed information about distribution of thermal and physiological properties, the averaged values of these parameters, obtained in anatomical investigation, are usually used. In such cases, the limb is divided into a few layers and in each layer all necessary parameters are considered as constant. The step variation of these parameters occurs at the interface between two adjacent layers. Generally, the limb can be divided into one layer (i.e. homogeneous tissue) or two layers (i.e. core and shell) or four layers (i.e. core, muscle, fat, skin), giving rise to the so-called 'one-layer', 'two-layer' and 'four-layer' models—the above-mentioned governing equations are applicable for each layer. The simplest case is that the limb is approximated as a homogeneous layer and the corresponding properties are the averaged values over the whole limb.

Both the arterial and venous blood flows flow through the vessels and disperse through the tortuous capillary beds. To describe the arterial and venous blood flows, the hydraulic diameter $d^* = 4\times$ void volume/surface area $= 4\varepsilon/\sigma(1-\varepsilon)$ for each flow is introduced. With definition of the following dimensionless parameters and variables:

$$\bar{x}=\frac{x}{L}\quad \bar{r}=\frac{r}{R_{MAX}}\quad \bar{\tau}=\frac{\tau}{\tau_M}\quad \Theta=\frac{\langle T\rangle-T_r}{T_{set}-T_r}$$

$$\beta=\frac{L}{R}\quad \mu_a=\frac{R^2\sigma_a^2(1-\varepsilon_a)}{4\varepsilon_a}\quad \mu_v=\frac{R^2\sigma_v^2(1-\varepsilon_v)}{4\varepsilon_v}$$

$$Pe_a=\frac{\varepsilon_a(\rho c_p)_a u_a L}{k_a^*}\quad Pe_v=\frac{\varepsilon_v(\rho c_p)_v u_v L}{k_v^*}$$

$$Nu_a=\frac{h_a d_a^*}{k_a^*\sigma_a}\quad Nu_v=\frac{h_v d_v^*}{k_v^*\sigma_v}$$

$$\bar{q}_m = \frac{q_m(1-\varepsilon)}{k_s^a} \quad \alpha_a = \frac{k_a^*}{k_s^a}$$

$$\alpha_v = \frac{k_v^*}{k_s^a} \quad Fo_a = \frac{\alpha_a \tau_M}{L^2}$$

the previously proposed governing differential equations are rewritten in dimensionless forms:

$$\frac{1}{Fo_a}\frac{\partial \Theta_a}{\partial \bar{\tau}} + Pe_a \frac{\partial \Theta_a}{\partial \bar{x}} = \frac{\partial^2 \Theta_a}{\partial \bar{x}^2} + Nu_a \mu_a (\Theta_s - \Theta_a) \tag{6}$$

$$\frac{a_a}{a_v Fo_a}\frac{\partial \Theta_v}{\partial \bar{\tau}} - Pe_v \frac{\partial \Theta_v}{\partial \bar{x}} = \frac{\partial^2 \Theta_v}{\partial \bar{x}^2} + Nu_v \mu_v (\Theta_s - \Theta_v) \tag{7}$$

$$\frac{a_a}{a_s Fo_a}\frac{\partial \Theta_s}{\partial \bar{\tau}} = \beta^2 \frac{1}{\bar{r}}\frac{\partial}{\partial \bar{r}}\left(\bar{r}\frac{\partial \Theta_s}{\partial \bar{r}}\right) + \frac{\partial^2 \Theta_v}{\partial \bar{x}^2} + Nu_a \mu_a \alpha_a (\Theta_a - \Theta_s) + Nu_v \mu_v \alpha_v (\Theta_v - \Theta_s) + \bar{q}_m. \tag{8}$$

The physical meanings of some parameters appearing in these equations have been discussed in ref. [5]. These equations are valid for each layer of the limb because the properties are assumed to be constant within each layer. The general forms of the initial conditions are as follows:

$$\Theta_a(\bar{x}, 0) = g_a(\bar{x})$$

$$\Theta_v(\bar{x}, 0) = g_v(\bar{x})$$

$$\Theta_s(\bar{x}, \bar{r}, 0) = g_s(\bar{x}, \bar{r}). \tag{9}$$

The boundary conditions are more complicated, which depend upon energy exchange between the limb and environment. Heat can be transferred from the surface of the limb to the environment and/or from the environment to the surface of the limb. The following boundary conditions are given:

$$\text{at } \bar{r} = 0 \quad \frac{\partial \Theta_s}{\partial \bar{r}} = 0 \tag{10}$$

at $\bar{r} = 1$

$$-\frac{\partial \Theta_s}{\partial \bar{r}} = Bi_c(\Theta_s - \Theta_f) + Bi_r(\Theta_s - \Theta_r) + \bar{E}_{evap} - \bar{E}_{sup}$$

$$Bi_c = \frac{h_c R}{k_s} \quad Bi_r = \frac{h_r R}{k_s}$$

$$\bar{E}_{evap} = \frac{E_{evap} R}{k_s (T_{set} - T_r)}$$

$$\bar{E}_{sup} = \frac{E_{sup} R}{k_s (T_{set} - T_r)} \tag{11}$$

at $\bar{x} = 0$

$$\Theta_a = \Theta_{bl} \tag{12}$$

$$\frac{\partial \Theta_v}{\partial \bar{x}} = 0 \tag{13}$$

$$\frac{\partial \Theta_s}{\partial \bar{x}} = \beta Nu_a \alpha_a H_a (\Theta_s - \Theta_a) + \beta Nu_v \alpha_v H_v (\Theta_s - \Theta_v)$$

$$H_a = \frac{L\varepsilon_a}{d_a^*} \quad H_v = \frac{L\varepsilon_v}{d_v^*} \tag{14}$$

at $\bar{x} = 1$

$$\Theta_a = \Theta_v \tag{15}$$

$$\frac{\partial \Theta_a}{\partial \bar{x}} = -\frac{k_v^*}{k_a^*}\frac{\partial \Theta_v}{\partial \bar{x}} \tag{16}$$

$$-\frac{\partial \Theta_s}{\partial \bar{x}} = Bi_c(\Theta_s - \Theta_f) + Bi_r(\Theta_s - \Theta_r) + \bar{E}_{evap} - \bar{E}_{sup}. \tag{17}$$

With the assumption of zero porosity on the outermost skin surface (no blood flow to the vicinity) the thermal conductivity k_s of the tissue, rather than the apparent conductivity k_s^a, is used for defining the Biot number *Bi* in the boundary conditions of equations (11) and (17). Both these conditions are versatile and take all possible modes of heat exchange on the surface into account. Practically, it is not necessary that all these heat exchange manners appear simultaneously. If it is necessary to take the evaporative heat loss by sweat into account, this type of heat flux may be calculated according to

$$E_{evap} = n_w A_{wskin} \gamma_{fg} = h_m [\rho_{w,sat}(T_{wskin}) - \phi_f \rho_{f,sat}(T_f)] A_{wskin} \gamma_{fg}$$

where the mass transfer coefficient h_m can be calculated from the convective heat transfer correlation by means of the heat and mass transfer analogy; A_{wskin} is the wetted skin surface. Here it is assumed that the relative humidity on the wetted skin surface is equal to one.

If it is necessary to include thermal dispersion of the arterial blood at the point where the blood enters the limb, the Dankenwerts' type of boundary condition $\Theta_{bl} - \Theta_a = -1/Pe_a \partial\Theta/\partial\bar{x}$ should be substituted for the above-mentioned condition of equation (12). A simpler alternative to the boundary condition of equation (14) for the tissue may be $\Theta_s = (\Theta_a + \Theta_v)/2$. According to the anatomical knowledge of the circulatory system, the continuous conditions of equations (15) and (16) are suggested for both the arterial and venous blood flows at the end of the limb. In cases where the limb is divided into separate layers, the additional boundary conditions in the radial direction for the tissue should be given at the interface between two adjacent layers. These continuous interfacial conditions are as follows:

$$\Theta_{s,j}(\bar{x}, \bar{R}_j, \bar{\tau}) = \Theta_{s,j+1}(\bar{x}, \bar{R}_j, \bar{\tau}) \quad (18a)$$

$$k^a_{s,j} \left.\frac{\partial \Theta_{s,j}}{\partial \bar{r}}\right|_{\bar{r}=\bar{R}_j} = k^a_{s,j+1} \left.\frac{\partial \Theta_{s,j+1}}{\partial \bar{r}}\right|_{\bar{r}=\bar{R}_j}. \quad (18b)$$

So far the thermal model of the limb has been established—it is suitable for either the naked or the clothed limb. Generally, the effect of clothes is approximately taken into account by defining the insulation I of a clothing system [11, 12]. The SI unit of I is called 'clo' and 1 clo is equal to 0.155 m^2 K W^{-1}; with this parameter, the difference between the skin and ambient temperatures can be approximately assessed. If the effect of clothes needs to be more accurately considered, two additional layers in which there is no blood flow and no metabolic heat generation can be added directly to the previously proposed thermal model; one for the still air layer for the human body in the environment or the still water layer for the human body immersed in water and the other for the porous clothes. Only heat conduction occurs in these two layers. For the still air or water layer between the skin surface and the inner surface of the clothing, heat flow is controlled by the conduction equation:

$$\frac{a_a}{a_{sw} Fo_a} \frac{\partial \Theta_{sw}}{\partial \bar{\tau}} = \beta^2 \frac{1}{\bar{r}} \frac{\partial}{\partial \bar{r}} \left(\bar{r} \frac{\partial \Theta_{sw}}{\partial \bar{r}} \right) + \frac{\partial^2 \Theta_{sw}}{\partial \bar{x}^2} \quad (19)$$

and the clothing layer may be modeled as a porous medium with local thermal equilibrium and heat transport is expressed by

$$\frac{a_a}{a_{cl} Fo_a} \frac{\partial \Theta_{cl}}{\partial \bar{\tau}} = \beta^2 \frac{1}{\bar{r}} \frac{\partial}{\partial \bar{r}} \left(\bar{r} \frac{\partial \Theta_{cl}}{\partial \bar{r}} \right) + \frac{\partial^2 \Theta_{cl}}{\partial \bar{x}^2} \quad (20)$$

where thermal diffusivity a_{cl} is a function of thermal properties of the clothing material and of the fluid perfused within the clothes. Correspondingly, the boundary condition (11) should be replaced by the interfacial conditions (18) between the outermost skin and the still fluid layer and be shifted to the outside of the clothes.

NUMERICAL ALGORITHM

The previously proposed governing equations are conjugated and the finite-difference method is used to find the transient response of the human limb to external stimulus. For numerical computation, the implicit finite difference representation is applied to these differential equations and the alternating direction implicit (ADI) method is employed for finite-difference representation of equation (8) because it gives rise to tridiagonal matrices like a one-dimensional problem for either of the two alternating directions and the computation scheme is very efficient. The upwind-difference scheme is applied to the convection term in equations (6) and (7) to maintain a stable numerical solution. By means of Patankar's expression [13], the finite-difference representation of these equations is as follows:

$$a_{aP}\Theta_{aP} = a_{aE}\Theta_{aE} + a_{aW}\Theta_{aW} + b_a \quad (21)$$

$$a_{vP}\Theta_{vP} = a_{vE}\Theta_{vE} + a_{vW}\Theta_{vW} + b_v \quad (22)$$

$$a_{sP}\Theta_{sP} = a_{sE}\Theta_{sE} + a_{sW}\Theta_{sW} + a_{sS}\Theta_{sS} + a_{sN}\Theta_{sN} + b_s \quad (23)$$

where the coefficients a_{ij} and b_i may assume different values for the tissue and the arterial and venous blood flows. For the given boundary conditions, one has the similar finite-difference expressions.

If the limb is divided into several layers with different thermal and physiological properties, the discretization method is assumed such that a control-volume face nearest to the boundary of a layer is exactly the interface between two adjacent layers. In this way, the discontinuity of the properties in a control-volume is avoided. The so-called harmonic value [13] of the conductivity is used for evaluating the interface conductivity. For convenience of numerical computation, the program can automatically distinguish the order number of the discretized grid points nearest to the interface for the given dimensions.

Since these finite-difference equations are conjugated to each other, iteration is needed for each time step, although it is not necessary to carry out iterative computation for the ADI algorithm itself. For the temperature computation of the tissue as well as the arterial and venous blood flows, the convergent criterion is

$$|\Theta_i^{k+1} - \Theta_i^k| / |\Theta_i^{k+1}| \leqslant 10^{-5} \quad (24)$$

where Θ_i may be Θ_s, Θ_a or Θ_v. The solution region (the limb) can be discretized into many small meshes. The following computation is related to an arm with length $L = 0.7272$ m and radius $R = 0.0556$ m and it is discretized into 101×81 meshes.

Some necessary anatomical and physiological properties are referred to in refs. [1, 4, 14] and are listed in Tables 1 and 2. The basic data listed in Table 2 are the weighted means of the properties listed in Table 1 over the related regions and the weight is the relative thickness of each layer. Practically, there may be different ways to average them from the distributed parameters. The densities and specific heat capacities of the arterial and venous blood flows are given as $\rho_a = \rho_v = 1059$ kg m^{-3} and $c_{pa} = c_{pv} = 3850$ J kg^{-1} K^{-1}, respectively. The apparent conductivities of the arterial and venous blood flows are assumed as $k_a^* = k_v^* = 0.64$ W m^{-1} K^{-1}. Since there is a shortage of porosity and specific surface area of the tissue and the interstitial heat transfer coefficient at present, such parameters may be estimated approximately from the available data for other porous media [15, 16]. If the blood flow through the porous tissue is assumed to be in the fully developed flow regime, the Nusselt number values may be given as $Nu_a = Nu_v = 4.93$ [16] which is independent of the flow Reynold's number and axial location.

Table 1. Basic data of the four-layer arm model

	Core	Muscle	Fat	Skin
Radius [m]	0.03109	0.05102	0.05319	0.05560
Density [kg m^{-3}]	1357	1085	920	1085
Specific heat capacity [J kg^{-1} K^{-1}]	1700	3800	2300	3680
Thermal conductivity [W m^{-1} K^{-1}]	0.75	0.51	0.21	0.47
Metabolic heat generation [W m^{-3}]	368.3	684.2	368.3	368.1

Table 2. Basic data of the two- and one-layer models

	Two-layer		One-layer
Layer	Core	Shell	Homogeneous tissue
Radius [m]	0.05102	0.05560	0.05560
Density [kg m^{-3}]	1250.8	1006.8	1230.7
Specific heat capacity [J kg^{-1} K^{-1}]	2520.3	3026.2	2562.0
Thermal conductivity [W m^{-1} K^{-1}]	0.656	0.347	0.631
Metabolic heat generation [W m^{-3}]	492.7	368.2	481.5

NUMERICAL EXAMPLES AND DISCUSSIONS

For computation of the first example it is assumed that the arm is initially in thermal equilibrium with the environment at 30°C and the tissue as well as the arterial and venous blood flows have a steady-state temperature distribution. The initial wind speed and relative humidity are set at 0.05 m s^{-1} and $\phi_f = 0.40$, respectively. The inlet temperature of the arterial blood is assumed as $T_{bl} = 37.3$°C. A new transient process begins with the environmental temperature 18°C and a new wind speed of 0.1 m s^{-1}. The computation consists of two steps; the first for the initial temperature distributions $g_a(\bar{x})$, $g_v(\bar{x})$ and $g_s(\bar{x}, \bar{r})$ which are determined by a steady-state programme; the second for the transient response of the arm subject to the given boundary conditions and initial temperature distributions.

The blood flow rate depends strongly upon the level of exercise. The Péclet number Pe appearing in the above-mentioned equations is directly controlled by the blood flow and the dispersion through the tissue. The approximation $Pe_a = Pe_v = 60$ may be chosen for the resting state [9]. The porosity ε and specific surface area σ depend upon such factors as the body temperature and interaction with the environment, as well as vasoconstrictor and vasodilator mechanisms. These parameters should be experimentally determined. To carry out the following computation in the case of shortage of experimental values, some estimated values are introduced by referring to the data related to similar porous media, which does not affect explanation of the applicability of the above model. In fact, the analysis [5] has shown that the temperature distribution within the limb is not sensitive to slight variation of these two parameters.

As pointed out previously, the multi-layer model is an approximation of the model with spatially distributed properties. Different division methods may result in different layer models, which relies on the average algorithm of the thermal, anatomical and physiological properties, to some extent. Generally, from the different layer models different temperatures are obtained. The deviation among the various layer models depends upon the original spatial distributions of the aforementioned properties. The initial temperature distributions of the arterial blood and the tissue at $r = 0$ are illustrated for the three different models in Fig. 1. The temperature distribution of the venous blood is not given because it is similar to that of the arterial blood. Obviously, the temperature profiles related to each model are different from each other. The difference between the one-layer and two-layer models is small compared to the four-layer model, since the various types of properties pertinent to the four-layer model are quite different from those in the one-layer or two-layer model and the differences between the properties related to the one-layer and two-layer models are remarkably small (as shown in Tables 1 and 2).

If the human body is suddenly exposed to a changed thermal environment from the initial state, the temperature distributions within the human body will change and the thermoregulatory system of the human body will function. The following figures show the passive temperature responses of the body subject to an external stimulus. The active thermoregulatory function is not taken into account during the computation of the first example because this article is mainly aimed at examining the applicability of the bioheat equation developed in ref. [5] and the difference among the distinct layer models. Only one of the thermoregulatory functions, sweating, can be treated by altering the boundary condition of equation (11) in the second example. Application of the bioheat equation to the whole human body will be involved in the future work, in which all active thermoregulatory

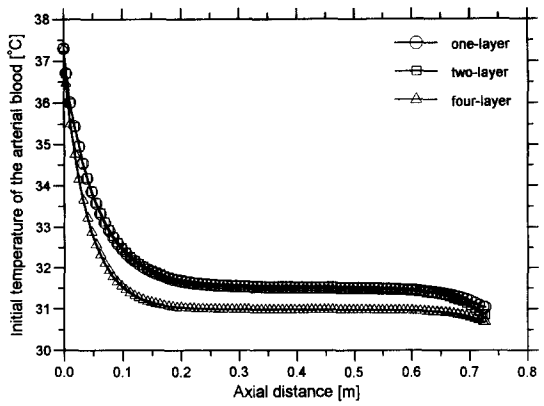

(a)

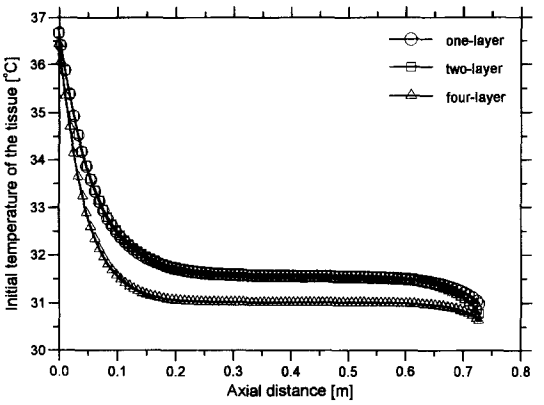

(b)

Fig. 1. The initial temperature distributions: (a) arterial blood flow, (b) tissue at $r = 0$.

functions of the human body will be taken into account. The curves in Fig. 2 reflect the temporal temperature profiles of the arterial and venous blood flows in the arm subject to the previously described external stimulus. As expected, these temperatures related to the various layer models are different from each other because of the different distributions of the properties which affect heat exchange between the blood and the tissue. The curves in this figure reveal that the countercurrent effect between the arterial and venous blood flows makes their temperature profiles approach each other. Comparison of these curves shows that the temperature profiles related to the arterial and venous blood flows are almost identical for each of these models. Further computation shows that with increasing Pe which corresponds to an increase in the blood flow or a decrease of thermal dispersion of the blood through the tissue, the temperature difference between these two blood flows becomes somewhat evident, but the countercurrent effect always makes these two temperature distributions converge with increasing flow length.

Figure 3 shows the transient response of the tissue temperature after 1800 s according to the three different layer models. These spatial distributions are different from each other because different discrete anatomical and thermal properties are inserted in each model. Figure 3(a) clearly represents the effect of the different properties in different layers. Comparing Fig. 3(a)–(c) one can find that the deviation between the one- and four-layer models is bigger than that between the one- and two-layer models or that between the two- and four-layer models. The one-layer model describes the effect of the mean values of the properties averaged over the layers and treats the arm as a homogeneous porous medium, but the four-layer model reveals the effect of the district distributions of these properties. The results obtained from the two-layer model may be considered as the intermediary between those from the one-layer model and those from the four-layer model. Since a layer may be very thin for the four-layer model, many grid points must be assumed in order to ensure that the spatial step thickness is smaller than that of any layer. Therefore, the four-layer model may cost much more computation time than the one-layer or two-layer model does. In view of computation time and accuracy, the two-layer model may be a good compromise.

The temperature distributions of the human body depend not only upon the local distributions of the afore-mentioned properties, but also on the boundary conditions. The second example illustrated in Figs. 4–6 includes all types of boundary conditions described in equation (11). Assuming that the human body is initially in a comfortable environment: the environmental temperature is 25°C, the relative humidity $\phi_f = 0.6$, the wind speed is 0.05 m s^{-1} and there is no irradiation from the sun, in this initial state the evaporative heat loss from the skin surface may be considered to be very low and entirely due to the diffusion of water vapour through the outermost skin surface. In this case the relative wetted surface area may be assumed as 0.06. The temperature profiles in the arm are initially computed for the steady-state. Then, the body is suddenly in a hot environment: the environmental temperature is 45°C, the relative humidity $\phi_f = 0.2$, the wind speed is 1.0 m s^{-1}, the arm is exposed to irradiation from the sun and the solar radiation is assumed as $E_{sup} = 258$ W m^{-2}. While the human body is exposed to a hot environment and sunburn, the heart rate and, consequently, the blood flow rates increase. The Péclet number may be assumed as $Pe = 150$. The heat load obtained by the body is regulated through sweating and the relative wetted surface area is assumed as 0.9. Figure 4 represents the spatial distributions of the arterial and venous blood temperatures at different times. With increasing exposure time, both these two blood temperatures rise. Under the boundary heat loads, the temperatures close to the end of the arm vary more steeply. Subjected to the effects of the initial temperatures and heat exchange between blood and tissue, the blood temperatures away from the end of the arm change slowly. This phenomenon indicates that the traditional lumped-parameter models [1, 4]

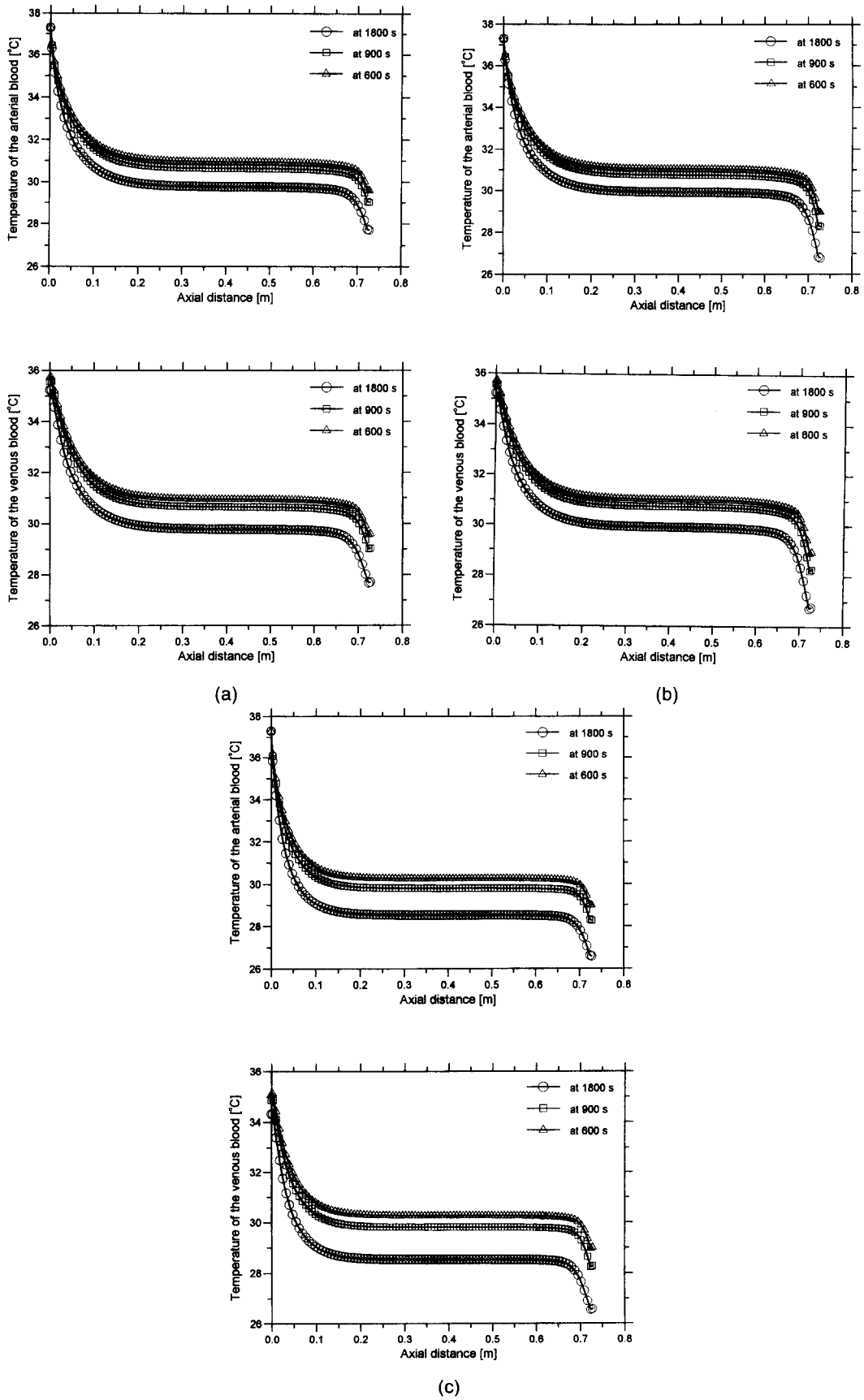

Fig. 2. The temporal temperature profiles of the arterial and venous blood flows: (a) one-layer model, (b) two-layer model, (c) four-layer model.

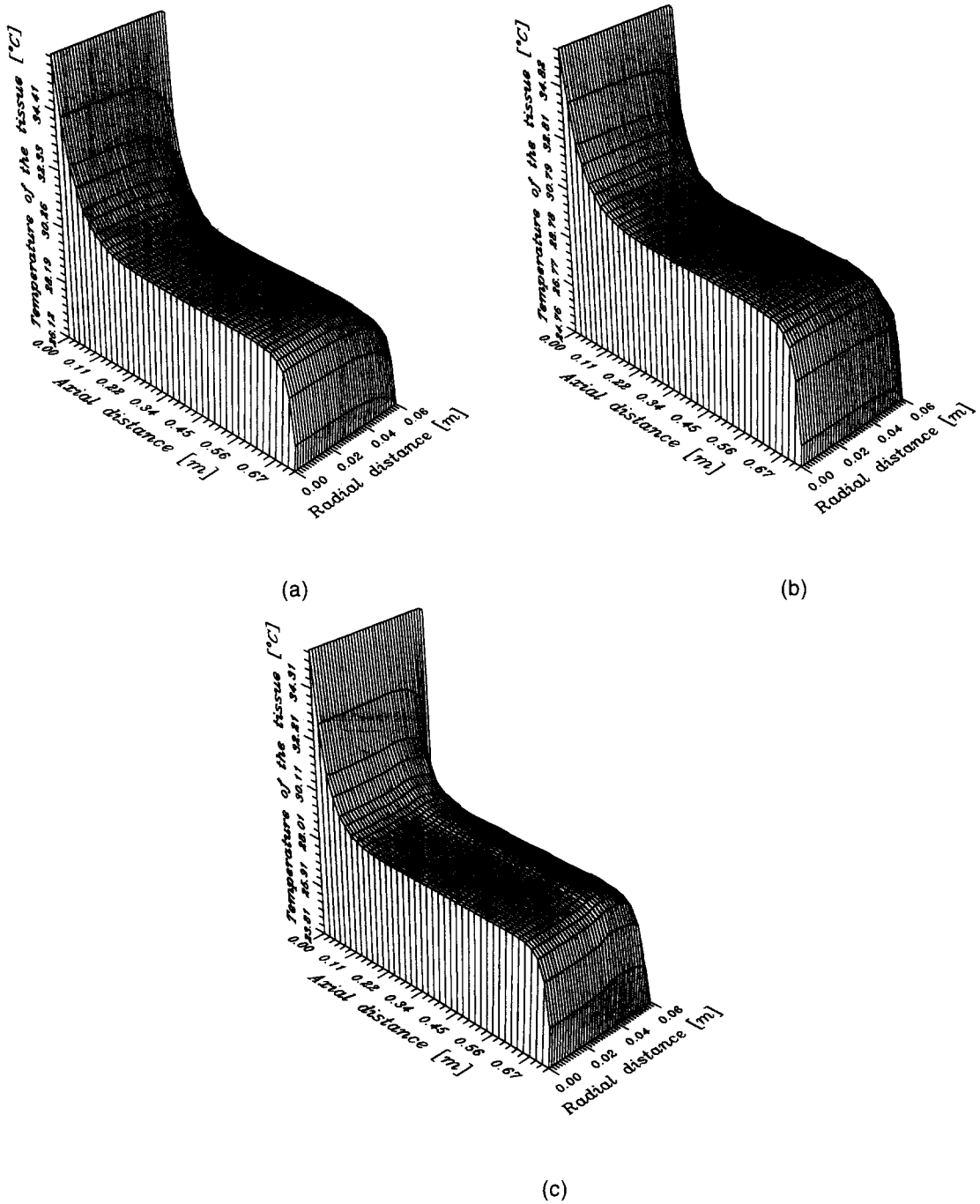

Fig. 3. The two-dimensional temperature distribution of the tissue at 1800 s: (a) one-layer model, (b) two-layer model, (c) four-layer model.

for the blood may not completely describe the temporal and spatial variation of the blood temperature. The two-dimensional temperature distribution of the tissue at 1800 s is illustrated in Fig. 5—the tissue temperature rises outwards. Figure 6(a) describes the axial distribution of the tissue temperature at the outermost skin surface and Fig. 6(b) the radial distribution of the tissue at $L/2$. All the curves in these figures show that the tissue temperature varies remarkably in both radial and axial directions and heat transfer in the tissue should be treated as a two-dimensional rather than a one-dimensional problem. In particular, the axial variation of the tissue temperature should not be neglected in an accurate bioheat model.

The previously described examples have testified to the applicability of the bioheat model developed in this article to the simulation of transient temperature distributions within a limb. The model encompasses such anatomical and thermal properties as the porosity, the specific surface area, the Péclet number,

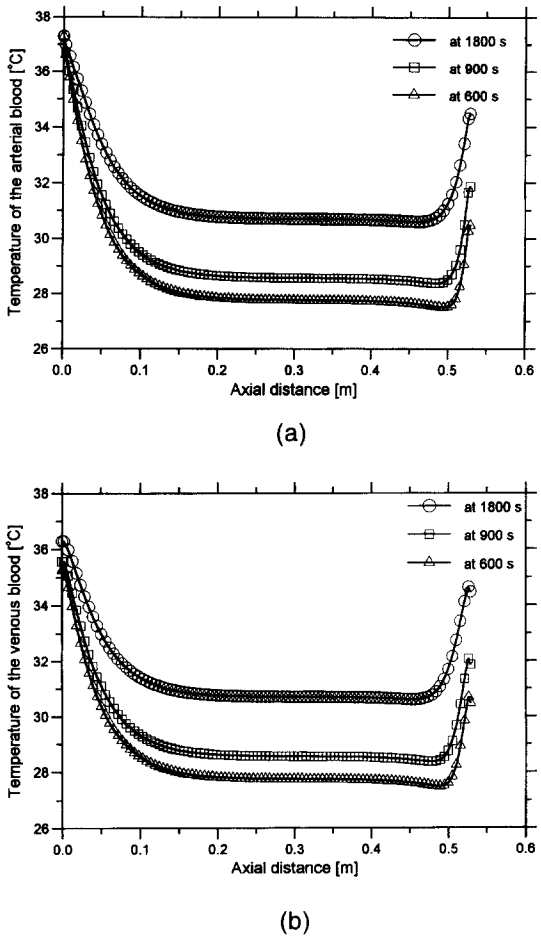

Fig. 4. The temporal temperature profiles of the arterial (a) and venous (b) blood flows within the arm suddenly subjected to a hot environment and sunburn from an initial comfortable environment.

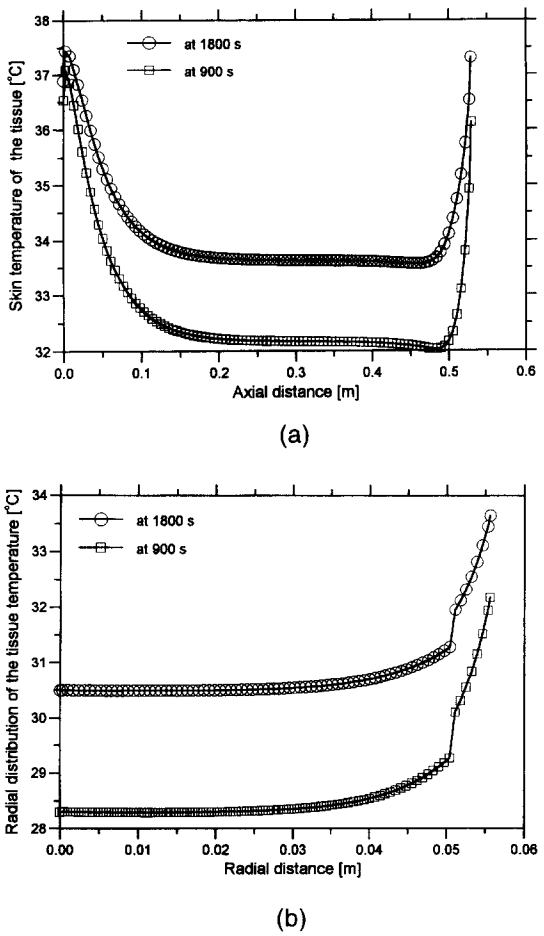

Fig. 6. The temporal temperature profiles of the tissue suddenly subjected to a hot environment and sunburn from an initial comfortable environment: (a) axial distribution on the outermost skin surface, (b) radial distribution at $L/2$.

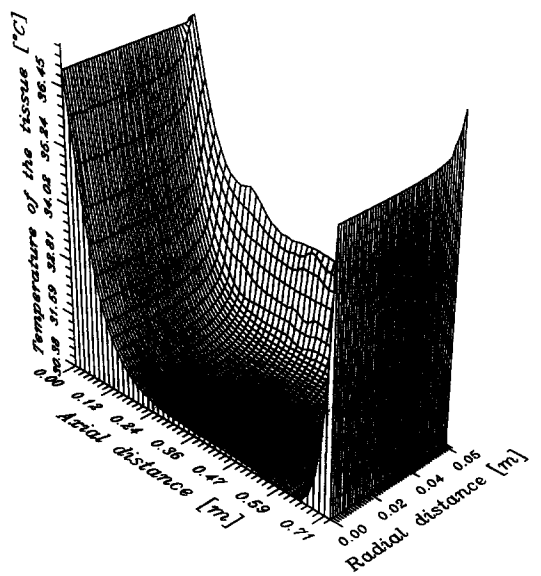

Fig. 5. The temperature distribution of the tissue of the arm suddenly subjected to a hot environment and sunburn from an initial comfortable environment.

the heat transfer coefficient, heat conductivities, specific heat capacities, blood flow rates and metabolic heat generation. Some are known and some unknown. In order to promote use of the model, it is necessary to experimentally determine the unknown properties.

CONCLUSIONS

The bioheat model developed on the basis of the heat transfer principle in porous media has been applied to the simulation of multidimensional transient behaviour of a limb subject to a sudden external heat stimulus. The examples include transition of a steady-state in a hot environment to a cold environment and transition of a steady-state in a comfortable environment to a hot environment subject to sunburn. The computation has indicated two-dimensional distribution of the tissue temperature. The axial variation of the blood and tissue temperatures and the countercurrent effect between them can not be neglected and should be included in the bioheat model.

Three different layer models have been discussed. The four-layer model evidently reveals the effect of the discrete properties, but it may cost much more computation time than the one-layer or two-layer model. For practical application, the two-layer may be preferable, especially for simulation of the whole human thermal system. To apply this model further the involved parameters need to be determined experimentally.

REFERENCES

1. Werner, J. and Webb, P., A six-cylinder model of human thermoregulation for general use on personal computers. *The Annals of Physiological Anthropology*, 1993, **12,** 123–134.
2. Pennes, H. H., Analysis of tissue and arterial blood temperature in the resting human forearm. *Journal of Applied Physiology*, 1948, **1,** 93–122.
3 Charny, C. K., Mathematical models of bioheat transfer. *Advances in Heat Transfer*, 1992, **22,** 19–155.
4. Arkin, H. and Shitzer, A., Model of thermoregulation in the human body, part I: the heat transfer model (the 'passive model'). Department of Mechanical Engineering, Technion, Haifa, Israel, 1984.
5. Xuan, Y. and Roetzel, W., Bioheat equation of the human thermal system. *Journal of Biomechanical Engineering* (submitted).
6. Weinbaum, S. and Jiji, L. M., A two phase theory for the influence of circulation on the heat transfer in surface tissue. In *Advances in Bioengineering*, ed. M. K. Wells. ASME, New York, 1979, pp. 179–182.
7. Weinbaum, S., Jiji, L. M. and Lemons, D. E., Theory and experiment for the effect of vascular microstructure on surface tissue heat transfer—part I anatomical foundation and model conceptuation. *Journal of Biomechanical Engineering*, 1984, **106,** 321–330.
8. Jiji, L. M., Weinbaum, S. and Lemons, D. E., Theory and experiment for the effect of vascular microstructure on surface tissue heat transfer—part II model formulation and solution. *Journal of Biochemical Engineering*, 1984, **106,** 331–341.
9. Song, W. J., Weinbaum, S. and Jiji, L. M., A theoretical model for peripheral tissue heat transfer using the bioheat equation of Weinbaum and Jiji. *Journal of Biomechanical Engineering*, 1987, **109,** 72–78.
10. Wissler, E. H., Comments on the new bioheat equation proposed by Weinbaum and Jiji. *Journal of Biomechanical Engineering*, 1987, **109,** 226–232.
11. Nishi, Y., Measurement of thermal balance of man. In *Bioengineering, Thermal Physiology and Comfort*, ed. K. Cena and J. A. Clark. Elsevier, Amsterdam, 1981.
12. Goldman, R. F., Evaluating the effects of clothing on the wearer. In *Bioengineering, Thermal Physiology and Comfort*, ed. K. Cena and J. A. Clark. Elsevier, Amsterdam, 1981.
13. Patankar, S. V., *Numerical Heat Transfer and Fluid Flow*. McGraw–Hill, New York, 1980.
14. Werner, J. and Buse, M., Temperature profiles with respect to inhomogeneity and geometry of the human body. *Journal of Applied Physiology*, 1988, **65,** 1110–1118.
15. Kaviany, L. H., *Principle of Heat Transfer in Porous Media*. Springer–Verlag, New York, 1991.
16. Tien, C. L. and Vafai, K., Convective and radiative heat transfer in porous media. In *Advances in Applied Mechanics*, Vol. 27, Academic Press, Boston, MA, ed. J. W. Hutchinson and T. Y. Wu, 1989, pp. 225–281.